ELSEVIER

Applied Catalysis A: General 169 (1998) 355–372

APPLIED CATALYSIS A: GENERAL

Synthesis of higher alcohols on copper catalysts supported on alkali-promoted basic oxides

Anne-Mette Hilmen, Mingting Xu, Marcelo J.L. Gines, Enrique Iglesia*

Department of Chemical Engineering, University of California at Berkeley, Berkeley, CA 94720, USA

Received 20 September 1997; received in revised form 13 January 1998; accepted 13 January 1998

Abstract

$K–Cu_yMg_5CeO_x$ and $Cs–Cu/ZnO/Al_2O_3$ are selective catalysts for the synthesis of alcohols from an H_2/CO mixture at relatively low pressures and temperatures. CO_2 produced in higher alcohol synthesis and water–gas shift (WGS) reactions reversibly inhibits the formation of methanol and higher alcohols by increasing oxygen coverages on Cu surfaces and by titrating basic sites required for aldol-type chain growth steps. Inhibition effects are weaker on catalysts with high Cu-site densities. On these catalysts, the abundance of Cu sites allows reactants to reach methanol synthesis equilibrium and maintain a sufficient number of Cu surface atoms for bifunctional condensation steps, even in the presence of CO_2. The addition of Pd to $K–Cu_{0.5}Mg_5CeO_x$ weakens CO_2 inhibition effects, because Pd remains metallic and retains its hydrogenation activity during CO hydrogenation. Basic sites on Mg_5CeO_x are stronger than on ZnO/Al_2O_3 and they are more efficiently covered by CO_2 during alcohol synthesis. K and Cs block acid sites that form dimethylether and hydrocarbons. Alcohol addition studies show that chain growth occurs predominantly by aldol-type addition of methanol-derived C_1 species to ethanol and higher alcohols, following the rules of base-catalyzed aldol condensations. The initial C–C bond formation required for ethanol synthesis, however, proceeds directly from CO, at least on $K–Cu_yMg_5CeO_x$ catalysts. A detailed kinetic analysis shows that chain growth probabilities are very similar on $K–Cu_yMg_5CeO_x$ and $Cs–Cu/ZnO/Al_2O_3$ catalysts. The growth probabilities of C_1 chains to ethanol and of *iso*-C_4 chains to higher alcohols are much lower than for other chain growth steps.

Keywords: Higher alcohols; Isobutanol; Methanol; Copper; Basic oxides; Potassium; Cesium

1. Introduction

The selective synthesis of methanol and isobutanol is attractive for the subsequent manufacture of methyl-*tert*-butyl-ether (MTBE) after isobutanol dehydration to form isobutene. An equimolar ratio of methanol to isobutanol would be preferred for MTBE synthesis. Methanol and higher alcohols can also be used for direct blending with hydrocarbon fuels. Mixtures of higher alcohols and methanol are preferred over pure methanol because of their higher water tolerance, reduced fuel volatility and lower vapor lock tendency, and also because their volumetric heating values are higher than for pure methanol [1].

The addition of alkali to Cu-based methanol synthesis catalysts leads to the formation of higher alcohols from H_2/CO mixtures [1,2]. Cs appears to be the best

*Corresponding Author. Fax: (510) 642-4778; e-mail: iglesia@cchem.berkeley.edu

0926-860X/98/$19.00
PII S0926-860X(98)00025-8

promoter for higher alcohol synthesis, but Rb and K also increase the selectivity to higher alcohols [3–5]. Potassium is often used because of its availability and low cost. The most studied catalysts for low-temperature higher alcohol synthesis are based on Cu and ZnO, often with Al_2O_3 or Cr_2O_3 as structural promoters that increase the surface area and prevent sintering [3–25]. Other Cu-based catalysts, such as K–$Cu_xMg_yCeO_z$ [26,27], have recently been shown to catalyze the synthesis of isobutanol at low temperatures. Li–Pd/ZrO_2–MnO_2–ZnO catalysts show very high isobutanol synthesis productivity at high temperatures (>673 K) and pressures (>10 MPa) [28].

The development of isobutanol synthesis catalysts that function at relatively low temperatures (<623 K) and pressures (<10 MPa) can decrease process costs and allow the use of large-scale slurry bubble column reactors. These reactors are well-suited for highly exothermic reactions because of their excellent heat removal properties. At low temperatures, however, currently available catalysts show high methanol selectivities, because methanol equilibrium, which is closely approached during higher alcohol synthesis [10,29], favors high methanol yields at low temperatures. Also, the kinetically-limited synthesis of higher alcohols becomes slower at low temperatures. As a result, the molar ratio of methanol to isobutanol is far from unity at low reaction temperatures.

The synthesis of methanol proceeds via reactions of CO_2 when using $CO/CO_2/H_2$ reactant mixtures and it is catalyzed by Cu surface atoms [30,31]. When CO_2-free feeds are used, the rate of methanol formation is not proportional to the Cu surface area [30]. In the absence of CO_2, basic sites are required along with Cu sites in methanol synthesis from H_2/CO mixtures [30]. Isobutanol synthesis requires the initial formation of methanol and higher linear alcohols and subsequent chain growth reactions leading to 2-methyl alcohols.

The formation of ethanol remains the least understood step in this reaction sequence. Recent results suggests that ethanol is formed directly from CO on K–$Cu_{0.5}Mg_5CeO_x$ catalysts [32], but via methanol condensation steps on Cs–Cu/ZnO/Al_2O_3 [20,32]. Although methanol is not involved in the formation of ethanol on K–$Cu_{0.5}Mg_5CeO_x$, it acts as a C_1 precursor in the synthesis of 1-propanol and 2-methyl-1-propanol from ethanol [33,34]. 2-Methyl-branched alcohols are formed by aldol condensation reactions; our recent studies have shown that these reactions require both Cu and basic sites [34]. Condensation steps occur on basic sites, but Cu sites appear to be required in order to remove hydrogen from the surface and to increase the rate of initial C–H bond activation steps. The addition of C_1 species to isobutanol is slow because of steric effects and also because isobutanol lacks the two α-hydrogens required for aldol condensation reactions.

Small amounts of CO_2 (~2%) promote methanol formation, but higher concentrations inhibit methanol synthesis [4,17]. The sensitivity to CO_2 depends on catalyst composition. Vedage et al. [4] have shown that methanol synthesis rates on Cu/ZnO increased when 2–6% CO_2 was added to H_2/CO mixtures, but much smaller rate enhancements were observed when such catalysts were modified with Cs. Steady-state oxygen coverages on Cu surfaces during methanol synthesis depend on the relative rates of addition and removal of oxygen during CO hydrogenation reactions [35]. At high CO_2 concentrations and in the presence of alkali, the rate of surface oxidation increases relative to reduction, leading to higher steady-state oxygen coverages and to a (reversible) decrease in the number of surface Cu metal atoms available for methanol synthesis steps. Similar trends have been reported for higher alcohol synthesis on alkali-modified methanol synthesis catalysts [9].

Our study focuses on catalysts consisting of Cu metal crystallites supported on basic oxides for the synthesis of methanol–isobutanol mixtures at low temperatures and pressures. This study includes studies of the effects of residence time, alloying, Cu-site density and crystallite size, and CO_2 and alcohol addition to H_2–CO reactants on reactions rates and selectivities, designed to probe reaction pathways required for isobutanol synthesis. It also includes some structural characterization data for K–$Cu_yMg_{5-}CeO_x$ and Cs–Cu/ZnO/Al_2O_3 catalytic materials.

2. Experimental

2.1. Catalyst preparation

$CuMgCeO_x$ samples were prepared by coprecipitation of mixed nitrate solutions with an aqueous solution of KOH (2 M) and K_2CO_3 (1 M) at 338 K at a

constant pH of 9 in a well-stirred and thermostated container. The precipitate was filtered, washed thoroughly with 300–500 cm^3 deionized water at 333 K, and dried at 353 K overnight. Dried samples were calcined at 723 K for 4 h in order to form the corresponding mixed oxides. Residual potassium in all dried samples measured by atomic absorption spectroscopy (AAS) was <0.1 wt% before alkali impregnation. $Cu/ZnO/Al_2O_3$ samples (Cu/Zn/Al molar ratio=54.8/30.1/15.1) were prepared following the same procedures as for $CuMgCeO_x$, except that the solution pH was held at 7.0 during precipitation and the dried powders were calcined at 623 K for 4 h [36]. K and Cs were added by incipient wetness using K_2CO_3 (0.25 M) and CH_3COOCs (0.25 M) aqueous solutions (K_2CO_3, Fisher Scientific, A.C.S. certified; CH_3COOCs, Strem Chemicals, 99.9%). The Pd-promoted catalyst was prepared by incipient wetness impregnation of $Cu_{0.5}Mg_5CeO_x$ with an aqueous solution of $Pd(NH_3)_2(NO_2)_2$, followed by air oxidation (0.5 K/min to 723 K, 4 h) before impregnation with K.

2.2. Catalyst characterization

Total surface areas were determined by N_2 physisorption at 77 K using a continuous flow Quantasorb surface-area analyzer (Quantachrome) and the BET analysis method. Bulk catalyst compositions were measured by atomic absorption spectroscopy (AAS). Copper metal surface areas were measured by N_2O (Matheson, ultrahigh purity) decomposition on pre-reduced samples at 363 K. A chemisorption stoichiometry of 0.5:1 $O:Cu_s$ was used in order to estimate Cu surface areas and dispersions [37,38].

The density of basic sites was measured by temperature-programmed desorption (TPD) and isotopic switch methods using CO_2 as a probe molecule [39]. Temperature-programmed CO_2 desorption (TPD) measurements consisted of pretreating the sample (50 mg) in flowing He ($\sim$100 cm^3/min) at 723 K for 0.3 h, followed by reduction in 5% H_2/He at 623 K for 0.5 h. The sample was then exposed to CO_2 (Cambridge Isotope Laboratories) for 0.15 h at room temperature, flushed with He in order to remove gas phase and weakly adsorbed CO_2, and the temperature increased up to 723 K at a rate of 0.5 K/s. The desorption profile of CO_2 was monitored continuously by mass spectrometry.

Exchangeable CO_2 was measured by a $^{13}CO_2/^{12}CO_2$ isotopic switch method. Pre-reduced samples were exposed to 0.1% $^{13}CO_2$/0.1% Ar/He (Cambridge Isotope Laboratories) at 573 K. After $^{13}CO_2$ reached a constant concentration in the effluent stream (0.5 h), the flow was switched to 0.1% $^{12}CO_2$/He (Cambridge Isotope Laboratories). Mass spectrometric analysis of $^{13}CO_2$ and Ar concentrations as a function of time after the isotopic switch were used to follow the decay in the concentration of $^{13}CO_2$ as it was replaced on the surface by $^{12}CO_2$. This method and the required data analysis protocols have been described in detail elsewhere [34,39].

2.3. High-pressure microreactor studies

High-pressure isobutanol synthesis studies were performed in a 1.27 cm i.d. stainless steel fixed-bed reactor with an axisymmetric thermowell (0.32 cm diameter). This reactor was held within a three-zone heated furnace in order to ensure uniform axial temperatures. The catalyst (2 g) was reduced in pure H_2 (Matheson, 99.99%) at 573–593 K and atmospheric pressure for 12 h before catalytic experiments were carried out at 4.5 MPa using synthesis gas mixtures (H_2/CO/Ar 0.45/0.45/0.1 mol.; Matheson: 99.99% CO, 99.99% Ar). Metal carbonyls were removed from synthesis gas streams using activated carbon (Sorb-Tech RL-13). H_2 was purified by passing through a catalytic purifier (Matheson, Model 64-1008). Traces of water were removed from H_2 and H_2/CO using molecular sieves (Matheson, Model 452:4A).

Analysis of the reactor effluent was carried out at regular intervals using a Hewlett–Packard 5890 II Plus gas chromatograph with thermal-conductivity (TCD) and flame-ionization (FID) detectors. Products and reactants were separated using a 5% phenyl–methyl–silicone capillary column (HP-5, 50 m, 0.32 mm diameter, 1.05 μm film thickness) and a packed column (Porapak Q, 1.8 m length, 0.32 cm diameter). The concentration of Ar, N_2, CO, and CO_2 in the effluent from the packed column was measured using TCD. FID was used to measure the concentrations of all organic compounds eluting from the capillary column.

CO_2 ($CO_2 : N_2$=1 : 1; Altair, 99.998% CO_2, 99.998% N_2) was added to the synthesis gas in order to examine the inhibiting effect of CO_2 on methanol

and isobutanol synthesis rates. CO_2 was introduced together with an internal standard (N_2) in a 1 : 1 molar ratio. The gas mixture was passed through a molecular sieve (Matheson, Model 452:4A) in order to remove trace amounts of water.

1-Propanol or ethanol were added using a liquid syringe pump (ISCO 500 D). Liquid propanol and ethanol reactants were degassed by flowing He for ~10 h before charging to the pump. After alcohol addition studies, the alcohol feed was stopped and the synthesis gas stream was kept flowing through the reactor in order to check recovery of activity and selectivity to the values measured before alcohol addition.

3. Results and discussion

3.1. Characterization

The characterization of CuMgCeO-type catalysts has been discussed previously [34] and will be summarized only briefly here. X-Ray diffraction (XRD) patterns showed separate MgO and CeO_x phases after air treatment at 723 K, suggesting that mixed $MgCeO_x$ oxides did not form [34]. CuO crystallites were not detected by XRD, consistent with small Cu crystallites or with Cu atoms present in a solid solution with CeO_2 [34]. Temperature-programmed reduction (TPR) studies showed that CeO_2 promotes the reduction of copper, apparently by providing hydrogen dissociation sites [34]. CeO_x addition to $Cu_{0.5}Mg_5O_x$ increased both the total surface area and copper dispersion (Table 1), suggesting that it also acts as a structural promoter [34]. TPR studies showed that potassium inhibits the reduction of copper oxide during H_2 treatment. This effect of alkali on copper is caused by inhibition of H_2 activation and by the strengthening of Cu–O bonds in CuO [34]. Copper dispersion decreased with increasing potassium loading (Table 1), because alkali species block surface Cu atoms and inhibit the reduction of CuO, and also because potassium decreases the surface area of Mg_5CeO_x supports.

3.2. Methanol synthesis

Methanol can be formed from synthesis gas via reaction (1). Methanol synthesis catalysts, however, also catalyze water–gas shift reactions (2). The stoichiometry of methanol synthesis from CO_2 is described by reaction (3).

$$CO + 2H_2 \rightarrow CH_3OH \quad (1)$$

$$CO + H_2O \rightarrow CO_2 + H_2 \quad (2)$$

$$CO_2 + 3H_2 \rightarrow CH_3OH + H_2O \quad (3)$$

The H_2/CO consumption ratio for methanol produced from CO is 2 : 1. Based on the stoichiometry of higher alcohol synthesis (reaction (4)), the H_2/CO consumption ratio for this reaction should also be 2 : 1. However, simultaneous WGS reactions modify this ratio, as illustrated by the combination of reactions (2) and (4) resulting in reaction (5).

Table 1
Composition, surface area, and basic site density of mixed metal oxides.

Sample	Cu loading (wt%)	K (Cs)[a] content (wt%)	BET surface area (m^2/g)	Cu[b] dispersion	Exchangeable CO_2 (at 573 K) (μmol/m^2)	CO_2 desorbed during TPD below 573 K[(mol/m^2]
$Cu_{0.5}Mg_5O_x$	13.2	0.2	118	0.06	—	—
$Cu_{0.5}Mg_5CeO_x$	7.7	0.1	167	0.23	1.2	0.62
$Cu_{0.5}Mg_5CeO_x$	7.7	1.0	147	0.14	2.3	0.64
$Cu_{0.5}Mg_5CeO_x$	7.7	3.5	62	0.06	5.2	0.65
$Cu_{7.5}Mg_5CeO_x$	49	1.2	92	0.05	3.3	0.91
$Cu/ZnO/Al_2O_3$	44	(1.2)	74	0.045	0.13	0.62
$Cu/ZnO/Al_2O_3$	44	(2.9)	62	0.05	1.1	0.72

[a] Bulk composition measured by atomic absorption. Values in parenthesis are for catalysts promoted with Cs instead of K.
[b] Dispersion calculated from the ratio of surface Cu (determined by N_2O decomposition at 363 K [37,38]) to the total number of Cu atoms in the catalyst.

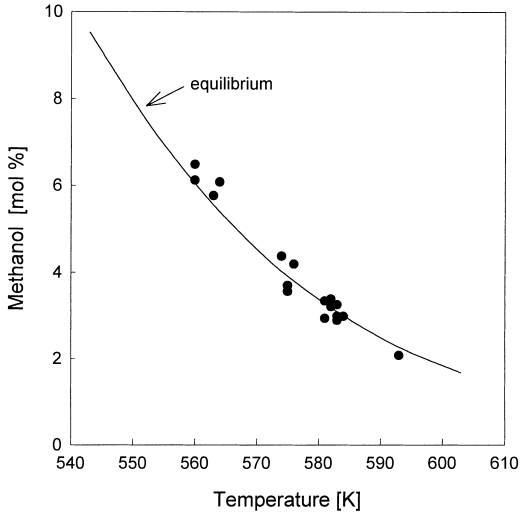

Fig. 1. Methanol mole fraction as a function of reaction temperature for Cs–Cu/ZnO/Al_2O_3 and K–$Cu_yMg_5CeO_x$ (4.5 MPa, 1500–6000 cm^3/g/h, H_2/CO=1. (———), equilibrium methanol mole fraction).

$$nCO + 2nH_2 \rightarrow C_nH_{2n+1}OH + (n-1)H_2O \quad (4)$$

$$(2n-1)CO + (n+1)H_2 \rightarrow C_nH_{2n+1}OH + (n-1)CO_2 \quad (5)$$

Thus, the H_2/CO usage ratio tends to decrease with increasing alcohol chain length, because the larger number of water molecules formed is subsequently converted to CO_2 and H_2 in reaction (2).

Fig. 1 shows how the measured mole fraction of methanol in the effluent stream varies with temperature for CO_2-free synthesis gas feeds. Calculated equilibrium methanol mole fractions, when methanol is produced by reaction (1) are also plotted in Fig. 1. The equilibrium mole fraction was calculated using temperature and pressure correlations for the equilibrium constant reported by Klier et al. [17] for non-ideal gas mixtures. The excellent agreement between measured and thermodynamic methanol concentrations shows that methanol synthesis from H_2–CO mixtures is at thermodynamic equilibrium at the reactor exit for the conditions of this study. As a result, the effect of changing process variables such as temperature, pressure, feed composition on methanol synthesis rates can be predicted accurately from thermodynamic data. When methanol yields are limited by equilibrium, synthesis rates become proportional to space velocity, because CO conversions to methanol remain constant with increasing bed-residence time, as illustrated for two catalysts in Fig. 2. The formation of higher alcohols is favored by higher temperatures and low space velocities. However, these conditions also favor the rapid equilibration of methanol synthesis reactions.

Methanol synthesis catalysts also catalyze WGS reactions and the latter reaction is likely to also approach equilibrium during higher alcohol synthesis. WGS reactions convert the water formed in the synthesis of higher alcohols, hydrocarbons, and dimethylether (DME), to CO_2 and H_2, while consuming CO, because thermodynamics favors the formation of CO_2 (K_{eq}=30) at our reaction conditions. Water can inhibit higher alcohol synthesis [40]; therefore its conversion to CO_2 may be desirable. Rapid WGS equilibration, however, makes it difficult to independently determine the inhibitory effect of CO_2 and H_2O on alcohol synthesis reactions, because the addition of CO_2 leads to an increase in both H_2O and CO_2 concentrations.

3.3. Bed-residence time effects

The effects of space velocity (bed-residence time) on alcohol synthesis rates and selectivities are shown in Fig. 2 for 1.2 wt% Cs–Cu/ZnO/Al2O3 and 1.0 wt% K–$Cu_{0.5}Mg_5CeO_x$ catalysts (data in Fig. 2b were taken from Ref. [34]). CO conversions should increase linearly with increasing bed-residence time at the low CO conversions of our study, unless the predominant methanol synthesis steps approach thermodynamic equilibrium. The observed decrease in the slope for the CO conversion curve with increasing bed-residence time in Fig. 2 reflects mainly the rapid approach to methanol synthesis equilibrium, as discussed above. It may also be influenced by an inhibition effect of CO_2 and H_2O on methanol synthesis, which becomes stronger as CO_2 and H_2O concentrations increase with increasing CO conversion. Isobutanol and higher alcohols form in secondary chain growth reactions, such as methanol carbonylation and aldol coupling reactions; therefore, their concentrations increase with increasing bed residence. C_2–C_3 alcohols are intermediate products that undergo further chain growth. As a result, their selectivity reaches a maximum value at intermediate residence times.

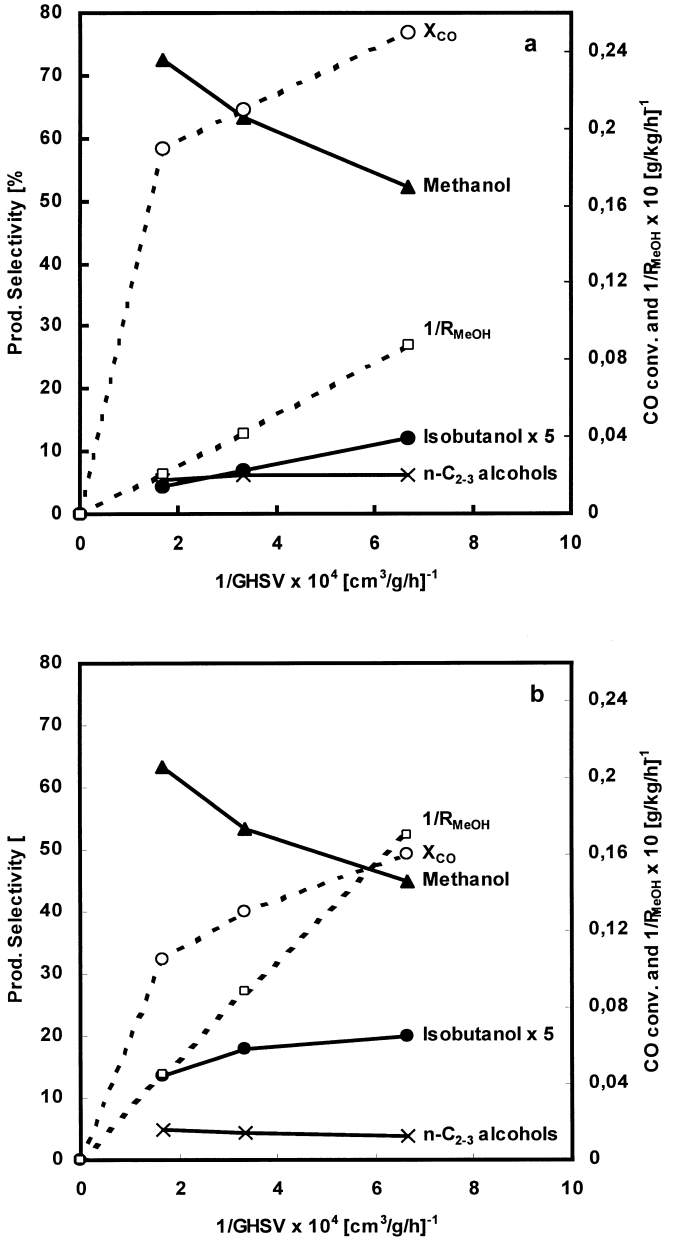

Fig. 2. CO conversion and product selectivities vs. space velocity on: a) 1.2 wt% Cs–Cu/ZnO/Al_2O_3 (563 K); b) 1 wt% K–$Cu_{0.5}Mg_5CeO_x$. (583 K), (4.5 MPa, CO/H_2=1, product selectivities are on CO_2-free basis).

Isobutanol is a kinetic end-product of aldol condensation chain growth processes, because it lacks the two α-hydrogens required for facile chain growth via aldol condensation pathways. Therefore, isobutanol selectivity increases monotonically with increasing residence time. This increase, however, is less marked on K–$Cu_{0.5}Mg_5CeO_x$ than on Cs–Cu/ZnO/Al_2O_3, because chain growth reactions are inhibited by CO_2 reaction products more strongly on K–$Cu_{0.5}Mg_5CeO_x$ than on Cs–Cu/ZnO/Al_2O_3. These effects are

discussed in more detail below. CO_2 appears to inhibit aldol-type coupling reactions during isobutanol synthesis on K-promoted $Cu_{0.5}Mg_5CeO_x$ catalysts. Weaker basic sites on Cs–Cu/ZnO/Al_2O_3 [34] appear to be less sensitive to CO_2 poisoning; as a result, isobutanol selectivities reach higher values than on K–$Cu_{0.5}Mg_5CeO_x$ as bed-residence time and CO conversion increase (Fig. 2(a) and (b)).

3.4. CO_2-addition to H_2-CO reactant mixtures

The presence of CO_2 in modest concentrations (1–2% mol) increases methanol synthesis rates on typical methanol synthesis catalysts (e.g. Cu/ZnO/Al_2O_3) [17]. High CO_2 concentrations (>10% mol) lead to surface oxidation and inhibit methanol synthesis on these catalysts [17]. Cs-modified methanol synthesis catalysts reach maximum rates at very low CO_2 concentrations (~2% mol) [3]. The relative rates of oxidation and reduction of Cu surface atoms determine the steady-state coverage of oxygen reaction intermediates during methanol synthesis. High concentrations of an oxidant, such as CO_2 or H_2O, will increase the rate of oxidation relative to reduction and lead to higher steady-state oxygen coverages and to fewer Cu surface atoms available for methanol synthesis. These Cu surface metal atoms catalyze methanol synthesis reactions of CO/CO_2/H_2 mixtures [30,31].

The details of CO_2 inhibition effects on methanol and isobutanol synthesis were examined by adding CO_2 to the H_2/CO reactants. As already mentioned, the effect of CO_2 cannot be separated from the effect of H_2O, because of the rapid equilibration of WGS reactions. CO_2 addition results are shown in Fig. 3 as the reciprocal of the methanol, ethanol, 1-propanol, and isobutanol synthesis rates vs. CO_2 concentration (data in Fig. 3(a) and (d) were taken from Ref. [34]). Typical Langmuir–Hinshelwood rate expressions (Eq. (6)) would lead to straight lines when data are plotted in this form, in agreement with the experimental data in Fig. 3.

$$r = r_0/(1 + KP_{CO2}) \quad (6)$$

Methanol synthesis rates on catalysts with high Cu contents decreased only slightly as CO_2 concentrations increased. Methanol synthesis rates on catalysts with lower Cu contents (1.0 wt% K–$Cu_{0.5}Mg_5CeO_x$) were more strongly inhibited by CO_2. These results are consistent with the more complete approach to methanol synthesis equilibrium on catalysts with higher Cu surface densities. Catalysts containing a higher density of Cu surface sites (e.g. 1.0 wt% K–$Cu_{7.5}Mg_5CeO_x$ and 2.9 wt% Cs–Cu/ZnO/Al_2O_3) can maintain equilibrium methanol concentrations even after a significant fraction of such sites are covered with oxygen adatoms during steady-state catalysis; therefore, the effect of CO_2 on methanol productivity is observed only at higher CO_2 concentrations. Equilibrium methanol concentrations vary slightly with CO_2 concentration [29]. This may account for the slight decrease in methanol yield observed even on catalysts with high Cu content. Catalysts containing fewer Cu sites (e.g. 1.0 wt% K–$Cu_{0.5}Mg_5CeO_x$) become unable to maintain methanol synthesis equilibrium conversions at lower CO_2 concentrations than catalysts with higher density of Cu sites.

The effects of CO_2 have not been as thoroughly studied in higher alcohol synthesis as in methanol synthesis. Tronconi et al. [40] observed decreased higher alcohol yields on K–$ZnCrO_x$ at 673 K when CO_2 (3–6%) was added to the H_2/CO feed. These authors proposed that water, formed from CO_2 in reverse WGS reactions, titrated alcohol synthesis sites. Elliot [13] showed that synthesis rates for higher alcohols on Cu/ZnO were increased by the addition of small amounts of CO_2 (6%). Calverley and Smith [9] observed that higher alcohol synthesis rates at 558 K reach a maximum at intermediate CO_2 concentrations (~4% CO_2) on Cu/ZnO/Cr_2O_3 (0–0.5 wt% K_2CO_3). They also reported that CO_2 inhibition effects became stronger with increasing alkali at concentrations corresponding to 0.5–4.0 wt% K_2CO_3.

Fig. 3(b)–(d) show reciprocal ethanol, 1-propanol, and isobutanol synthesis rates as functions of the average CO_2 partial pressure within the catalyst bed. The synthesis of higher alcohol synthesis on catalysts with low Cu content ($Cu_{0.5}Mg_5CeO_x$) was inhibited more strongly by CO_2 than on catalysts with higher Cu content. This may reflect a slight decrease in methanol concentrations with increasing CO_2 concentration (observed only on low-Cu content catalysts) and the reversible titration of both Cu and basic sites required for isobutanol synthesis. Although methanol appears not to be involved in the initial formation of ethanol on K–$Cu_{0.5}Mg_5CeO_x$ [32], it acts as a C_1 precursor in the synthesis of 1-propanol and isobuta-

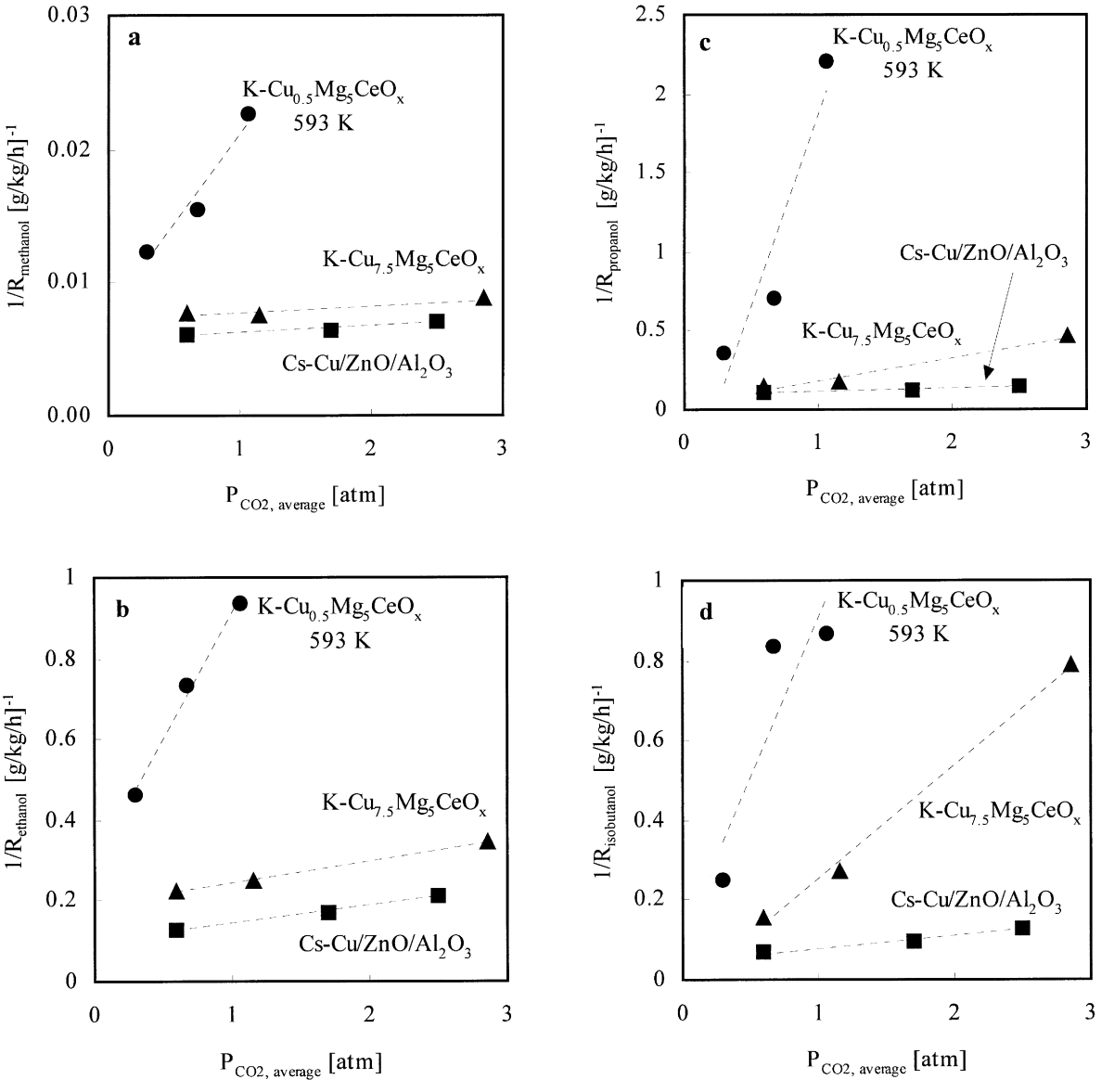

Fig. 3. Reciprocal methanol (a), ethanol (b), propanol (c) and isobutanol (d) productivity vs. average CO_2 partial pressure on 1 wt. % K-$Cu_{0.5}Mg_5CeO_x$, 2.9 wt. % Cs-Cu/ZnO/Al_2O_3 and 0.9 wt. % K-$Cu_{7.5}Mg_5CeO_x$. [583 K, 4.5 MPa,, 3000 cm^3/g/h, H_2/CO=1].

nol from ethanol. Aldol-type coupling reactions of alcohols require both Cu and basic sites [33]. Therefore, any blocking of surface Cu atoms by oxygen can also lead to a decrease in the rate of isobutanol synthesis, even when such blocking does not influence the rate of quasi-equilibrated methanol synthesis steps.

CO_2 inhibition of isobutanol synthesis steps can also reflect the reversible titration of basic sites on oxide surfaces by acidic molecules, such as CO_2. The inhibiting effect of CO_2 on isobutanol synthesis rates is greater on 0.9 wt% K–$Cu_{7.5}Mg_5CeO_x$ than on 2.9 wt% Cs–Cu/ZnO/Al_2O_3, possibly because of the stronger basicity of the former (inferred from CO_2

isotopic exchange and desorption rates [34]). On catalysts with low Cu content, chain growth reactions appear to be limited by the availability of minority Cu sites and, thus, reversible oxidation of surface Cu atoms by CO_2 decreases chain growth rates. At higher Cu contents, chain growth rates become limited by steps occurring on basic sites, which are blocked by CO_2 most effectively on the stronger basic sites available on the modified MgO materials. Basic sites on 0.9 wt% Cu–$Mg_{7.5}Mg_5CeO_x$ appear to be more sensitive to CO_2 than corresponding basic sites on 2.9 wt% Cs–Cu/ZnO/Al_2O_3, as previously shown from the faster CO_2 isotopic exchange rates on the latter [34].

3.5. Effect of Pd on K–$Cu_{0.5}Mg_5CeO_x$ catalysts

Isobutanol synthesis steps on catalysts with low Cu content appears to be limited by the hydrogenation/dehydrogenation function on these catalysts, especially at high CO_2 concentrations as Cu surfaces become increasingly covered with oxygen atoms. Pd metal is an excellent hydrogenation/dehydrogenation catalyst and its presence in small amounts may provide hydrogenation sites even at high CO_2 concentrations. Metal–oxygen bonds are weaker on PdO than on CuO, and, thus, Pd metal is less likely to oxidize than Cu–metal ($\Delta G \approx -170$ and -100 kJ/mol, respectively [41]). Pd has been used as catalyst for the synthesis of higher alcohols [28], but at much higher temperatures and pressures than those in this study.

Table 2 shows the effect of adding small amounts of Pd(0.25 %wt. Pd; Pd/Cu=0.02 at.) to 1 wt% K–$Cu_{0.5}Mg_5CeO_x$. CO conversions are similar on both 1 wt. % K-$Cu_{0.5}Mg_5CeO_x$ and 1 wt% K—0.25 wt% Pd–$Cu_{0.5}Mg_5CeO_x$ catalysts at all space velocities. Methanol synthesis rates are similar because methanol synthesis is near equilibrium on both catalysts.

Isobutanol synthesis rates are similar on the two catalysts only at high space velocities. Thus, Pd seems to have only a minor effect on the behavior of 1 wt% K–$Cu_{0.5}Mg_5CeO_x$, at low CO_2 concentrations. At lower space velocities, however, the Pd-promoted catalyst shows higher isobutanol synthesis selectivity and rates, suggesting that Pd weakens the inhibitory effects of CO_2. Pd crystallites appear to retain their hydrogenation activity as CO_2 concentrations increase and continue to provide hydrogen activation sites required for bifunctional alcohol coupling reactions at significantly higher CO_2 concentrations than on Pd-free catalysts. A horizontal line in Fig. 4 is expected for a differential reactor in the absence of product inhibition. The addition of Pd to the K–$Cu_{0.5}Mg_5CeO_x$ leads to a nearly horizontal line in Fig. 4.

3.6. Cu concentration effects on methanol and isobutanol synthesis rates

As shown previously, alcohol synthesis on catalysts with higher Cu concentrations is more weakly inhibited by CO_2 than on catalysts with lower Cu contents. Therefore, high Cu concentrations could lead to higher

Table 2
Productivities and selectivities on 0.25 wt% Pd–$Cu_{0.5}Mg_5CeO_x$ and $Cu_{0.5}Mg_5CeO_x$ (583 K, 4.5 MPa, $H_2/CO=1$)

Catalyst	(1 wt% K) 0.25 wt% Pd $Cu_{0.5}Mg_5CeO_x$			(1 wt% K) $Cu_{0.5}Mg_5CeO_x$		
Gas hourly space velocity (cm^3/g/h)	6000	3000	1500	6000	3000	1500
CO conversion (%)	10.6	13.1	15.8	9.9	11.8	14.7
CO conversion rate (mmol CO conv./g/h)	11.7	7.2	4.4	10.9	6.5	4.0
Methanol synthesis rate (g/kg/h)	236.2	130.4	64.5	227.8	122.2	65.0
Isobutanol synthesis rate (g/kg/h)	7.8	6.9	5.3	7.5	5.2	3.7
CO_2-selectivity [% C]	19.2	22.8	28.1	15.6	18.1	23.4
Carbon selectivities (% C; CO_2-free)						
Methanol	74.3	68.4	59.3	75.2	71.1	63.1
Ethanol	3.6	3.0	2.6	2.6	2.2	1.8
1-Propanol	3.7	4.1	4.1	3.6	3.3	3.0
Isobutanol	4.3	6.2	8.4	4.3	5.1	6.2
Dimethylether	1.0	1.2	1.6	4.0	4.5	6.8
Methyl acetate	0.7	0.9	1.3	1.1	1.0	1.2
Paraffins selectivity	6.3	8.7	13.3	4.7	6.5	9.9

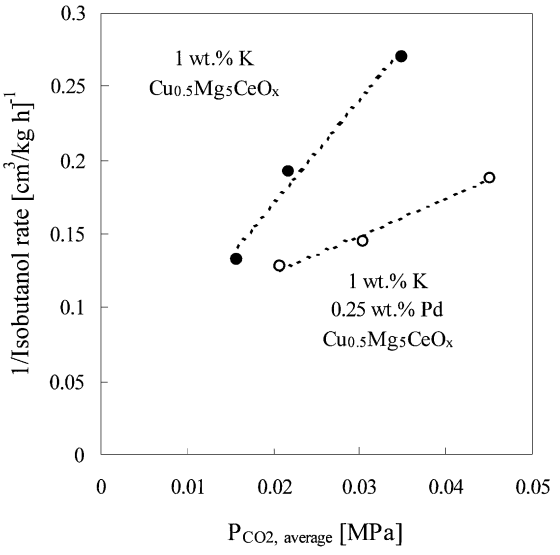

Fig. 4. Reciprocal isobutanol synthesis rate as a function of average CO_2 partial pressure on 1 wt% K–0.25 wt% Pd–$Cu_{0.5}Mg_5CeO_x$ and 1 wt% K–$Cu_{0.5}Mg_5CeO_x$ (583 K, 4.5 MPa, H_2/CO=1).

alcohol synthesis rates and selectivities. Table 3 shows CO conversion and product selectivities for 0.9 wt% K–$Cu_{7.5}Mg_5CeO_x$ and 1 wt% K–$Cu_{0.5}Mg_5CeO_x$.

At similar CO conversions, isobutanol synthesis rates are higher on the catalyst with high Cu content. Isobutanol selectivity, however, is lower on this catalyst. Isobutanol selectivity does not increase with decreasing space velocity on the catalyst with high Cu content (in contrast with the low Cu content catalyst). This reflects stronger inhibition effects at the very high CO conversions obtained with decreasing space velocity on this catalyst.

The 0.9 wt% K–$Cu_{7.5}Mg_5CeO_x$ catalyst has a higher selectivity to methyl acetate than the 1.0 wt% K–$Cu_{0.5}Mg_5CeO_x$ catalyst. Methyl acetate and other esters can be formed by Canizzaro-type condensations of two aldehydes, by reactions of surface carboxylates with formyl or formaldehyde, or by Tishchenko-type reactions of aldehyde species with surface alkoxides [3]. The latter reaction seems to be the most plausible pathway, in view of the expected presence of both aldehydes and surface alkoxides on our catalytic materials. The high selectivity to methyl acetate on the 0.9 wt% K–$Cu_{7.5}Mg_5CeO_x$ catalyst suggests that Cu sites promote the formation of methyl acetate, possibly by increasing aldehyde surface concentrations during higher alcohol synthesis.

Catalysts with high Cu concentrations show higher hydrocarbon selectivities than the catalysts with low Cu content at similar CO conversions. Hydrocarbons and dimethylether products require acid sites and hydrocarbon formation appears to require longer resi-

Table 3
Alcohol synthesis rates and selectivities on 0.9 wt% K–$Cu_{7.5}Mg_5CeO_x$ and 1 wt% K–$Cu_{0.5}Mg_5CeO_x$ (583 K, 4.5 MPa, H2/CO=1)

Catalyst	0.9 wt% K–$Cu_{7.5}Mg_5CeO_x$		1 wt% K–$Cu_{0.5}Mg_5CeO_x$
Gas hourly space velocity 9cm^3/g/h)	6000	1500	1500
CO conversion (%)	7.6	26.9	14.7
CO conversion rate (mmol CO conv./g/h)	19.4	7.4	4.0
Methanol synthesis rate (g/kg/h)	289	58	65
Isobutanol synthesis rate (g/kg/h)	9.5	2.7	3.7
Methyl acetate synthesis rate (g/kg/h)	19.3	9.3	1.3
Methanol turnover rate (mmol/mol Cu_s/s)	4.4	0.9	2.3
Isobutanol turnover rate (mmol/mol Cu_s/s)	0.06	0.02	0.06
CO_2 selectivity (% C)	27.5	40.5	23.4
Carbon selectivities (% C; CO_2-free)			
Methanol	57.4	35.5	63.1
Isopropanol	2.7	3.9	2.3
Ethanol	2.0	1.2	1.8
1-Propanol	3.1	1.7	3.0
Isobutanol	3.3	2.8	6.2
Paraffins	19.9	39.0	9.9
Methyl acetate	4.7	6.4	1.2
DME	0.7	1.0	6.8

dence and/or stronger acid sites than dimethylether. The high hydrocarbon selectivity on catalysts with high Cu concentrations reflects a higher acid density on these catalysts, possibly formed during the reduction of larger amounts of CuO than on catalysts with low Cu content. Hydrocarbon selectivity increases rapidly with decreasing space velocity on both catalysts, apparently because basic sites, but not acid sites, are inhibited by CO_2.

Increasing Cu concentrations leads to catalysts that are more resistant to CO_2 inhibition (Fig. 3). High CO_2 concentrations titrate basic sites on both high and low Cu catalysts, but high Cu catalysts retain a higher density of Cu sites required for bifunctional condensation reactions leading to alcohol chain growth. Therefore, higher isobutanol synthesis rates are obtained on high Cu catalysts at similar levels of CO conversion and CO_2 concentration.

3.7. Effect of Cs concentration on the synthesis of higher alcohols

The effect of increasing Cs concentration was studied on $Cu/ZnO/Al_2O_3$ catalysts. Methanol and higher alcohol synthesis rates were previously shown to reach a maximum with increasing alkali loading [3–5]. The amount required for optimum higher alcohol synthesis depends on the identity of the alkali added and on the density of acid sites that require titration on a given catalyst [22].

Table 4 shows alcohol synthesis rates on $Cu/ZnO/Al_2O_3$ catalysts promoted with Cs at two concentration levels (1.2 and 2.9 wt% Cs). Data reported by Nunan et al. [22] on similar $Cs–Cu/ZnO/Al_2O_3$ samples are also shown in Table 4. Increasing Cs concentrations from 1.2 to 2.9 wt% causes a significant increase in C_{2+}-alcohol synthesis rates and a decrease in dimethylether synthesis rate. Dimethylether is formed by condensation of methanol on acid sites. Alkali promoters, such as Cs, appear to titrate acid sites and to increase the density of basic sites on these catalysts (Table 1). This leads to lower dimethylether selectivity and higher alcohol selectivity as increasing amounts of Cs are added. At very high Cs concentrations, alcohol synthesis rates may ultimately decrease, because Cu-metal sites, required for chain growth, can also be titrated by Cs species.

Table 4
Higher alcohol synthesis on Cs-promoted $Cu/ZnO/Al_2O_3$ catalysts.

	Ref. [22]	This study	This study
Cs (wt%)	4.3[1]	1.2	2.9
Cu (wt%)	35	44	44
Temperature (K)	583	583	580
Pressure (MPa)	7.6	4.5	4.5
H_2/CO ratio	0.45	1	1
Gas hourly space velocity ($cm^3/g/h$)	5330	6000	6000
CO conversion (%)	—	15.0	15.4
Synthesis rate (g/kg/h)			
Methanol	405.0	269.6	342.3
Ethanol	12.6	12.0	16.1
1-Propanol	6.1	6.4	21.9
1-Butanol	5.5	0.8	0.3
2-Methyl-1-propanol	9.4	8.1	20.3
Methyl formate	10.4	1.3	0.4
Methyl acetate	3.4	13.8	4.2
Dimethylether	—	21.3	5.7
Hydrocarbons	13.9	12.9	6.2

[1] Calculated using data from Ref. [22].

Higher Cs concentrations also lead to lower methyl acetate formation rates, suggesting that Cs addition favors aldol condensation reactions over esterification reactions or that Cs promotes the conversion of acetate to ethanol, in contrast with earlier reports [5], which found that selectivities to esters and alcohols followed similar trends. Our results are consistent with the involvement of similar intermediates in esterification and aldol condensation steps; species such as adsorbed acetaldehyde are likely to participate both in methyl acetate formation and in 1-propanol formation. The decrease in methyl acetate synthesis rate and the increased isobutanol synthesis rate at high Cs concentrations suggest that Cs selectively promotes aldol-coupling reactions.

3.8. Alcohol addition to H_2–CO reactants

Ethanol and 1-propanol were added to the H_2/CO feed in order to probe chain growth pathways in higher alcohol synthesis. Isotopic tracer studies of ethanol reactions on $K–Cu_{0.5}Mg_5CeO_x$ catalysts [33,34] have shown that ethanol self-condensation reactions produce *n*-butyraldehyde, acetone, methylethyl ketone and 2-pentanone, which form 1-butanol, isopropanol, 2-butanol and 2-pentanol, respectively, at conditions

Table 5
Ethanol and 1-propanol addition on 2.9 wt% Cs–Cu/ZnO/Al_2O_3 (583 K, 4.5 MPa, 6000 cm^3/g cat/h, H_2/CO/Ar/C_2H_5OH =44.5/44.5/0.1/0.02 and H_2/CO/Ar/C_3H_7OH =44.5/44.5/0.1/0.01)

	None	Ethanol	None	Propanol	None
CO conversion (%)	15.4	14.8	14.8	14.2	14.3
Selectivities (CO_2-free) (% C)					
Methanol	67.6	67.5	69.2	69.9	71.0
Ethanol	4.4	12.2	4.3	3.5	4.2
1-Propanol	6.9	21.6	7.2	24.3	7.0
2-Propanol	0.7	2.8	0.6	1.1	0.6
2-Methyl-1-propanol	6.9	14.8	6.3	28.6	5.9
1-Butanol	1.0	2.9	1.0	2.0	0.9
1-Pentanol	0.3	1.2	0.3	1.4	0.2
1-Hexanol	0.2	0.6	0.2	0.5	0.2
2-Methyl-1-butanol	1.2	2.3	1.1	1.4	1.0
2-Methyl-1-pentanol	0.9	1.6	0.8	1.5	0.8
2-Methyl-1-hexanol	0.5	0.8	0.4	0.5	0.4
Methyl acetate	1.1	1.6	1.0	0.6	0.7
Dimethylether	0.8	0.3	0.7	0.5	0.6

typical of CO hydrogenation reactions. Isotopic tracer studies of methanol–acetaldehyde reactions have shown that propionaldehyde and 1-propanol are formed by condensation of methanol-derived C_1 species with acetaldehyde; isobutyraldehyde and isobutanol are formed by a similar C_1 addition to propionaldehyde [33,34].

Table 5 shows product selectivities on 2.9 wt% Cs–Cu/ZnO/Al_2O_3 catalysts when ethanol was added to H_2/CO reactants. The molar concentration of ethanol in the feed was about 25% of the methanol concentration in the reactor effluent. The selectivity to 1-propanol increases when ethanol is added, as expected from its formation via C_1 addition to C_2 intermediates. 1-Propanol can be formed both by aldol coupling and by linear chain growth (carbonylation) pathways. The selectivity to isobutanol also increases when ethanol is added. Isobutanol is formed only by C_1 addition to 1-propanol (or propionaldehyde). 1-Butanol selectivity also increased; 1-butanol can be formed by linear chain growth pathways or by ethanol aldol self-condensation pathways. Ethanol self-condensation can also lead to 2-propanol (after retro-aldol reactions) and 2-butanol. Increased selectivity for 2-propanol shows that self-condensation does occur, and that 1-butanol is predominantly formed by ethanol aldol self-condensation instead of linear chain growth pathways. The selectivity to 1-pentanol and 1-hexanol also increases. 1-Pentanol can be formed by condensation of ethanol with propanol or by linear chain growth of 1-butanol. 1-Hexanol is formed by condensation of ethanol with 1-butanol or by linear chain growth of 1-pentanol.

Table 5 shows the effect of adding 1-propanol to the H_2/CO feed. The molar concentration of 1-propanol in the feed was 20% of the methanol concentration in the reactor effluent. The large increase in isobutanol selectivity during 1-propanol addition confirms that isobutanol is formed predominantly by aldol-type C_1 addition to C_3 species derived from 1-propanol. The slight increase in 1-butanol selectivity during 1-propanol addition shows that minority linear chain growth pathways are available on Cs–Cu/ZnO/Al_2O_3. The ratio of the increase in isobutanol selectivity to the increase in 1-butanol selectivity when propanol is added shows that aldol condensation pathways are ca. 22 times faster than linear chain growth steps on 2.9 wt% Cs–Cu/ZnO/Al_2O_3 at the conditions of our study.

Table 6 shows the effect of adding 1-propanol to the H_2/CO feed on a 1.2 wt% K–$Cu_{7.5}Mg_5CeO_x$ catalyst. The ratio of the increase in isobutanol selectivity to the increase in 1-butanol selectivity on this catalyst is somewhat lower (∼9) than for the 2.9 wt% Cs–Cu/ZnO/Al_2O_3, but aldol-type C_1 addition steps remain the predominant chain growth pathway on K–$Cu_{7.5}Mg_5CeO_x$ catalysts.

Table 6
1-Propanol addition on 1.2 wt% K–$Cu_{7.5}Mg_5CeO_x$ (583 K, 4.5 MPa, 1500 cm^3/g cat/h, H_2/CO/Ar/C_3H_7OH =44.5/44.5/0.1/0.5)

	None	Propanol
CO conversion (%)	16.0	15.4
Selectivities (CO_2-free) (%)		
Methanol	60.6	53.3
Ethanol	2.8	1.2
1-Propanol	4.3	-
2-Propanol	3.0	1.3
2-Methyl-1-propanol	4.1	15.5
1-Butanol	0.2	1.5
1-Pentanol	0.1	1.0
1-Hexanol	0.2	0.4
2-Methyl-1-butanol	0.5	1.3
2-Methyl-1-pentanol	0.2	1.3

Aldol-type addition of C_1 species to linear alcohols leads to 2-methyl alcohols. The increase in 2-methyl-1-butanol and 2-methyl-1-pentanol is caused by the higher 1-butanol and 1-pentanol selectivity, respectively, when 1-propanol is added and also by the condensation of ethanol with propanol (leading to 2-methyl-1-butanol) and of two propanol molecules (leading to 2-methyl-1-pentanol). A reasonable estimate of the contribution of carbonylation reactions to chain growth can be obtained by assuming that all products that can form from 1-butanol (1-pentanol, 1-hexanol, 2-methyl-1-butanol, 2-methyl-1-pentanol, etc.), are actually formed only from 1-butanol. Even then, aldol condensation pathways are about eight times faster than linear chain growth on 2.9 wt% Cs–Cu/ZnO/Al_2O_3 catalysts.

Reaction pathways for the formation of observed products are shown in Fig. 5. These chain growth pathways are consistent with those proposed by Smith and Anderson [3], Smith et al. [23] and Breman et al. [6,7] for modified methanol synthesis catalysts. This scheme suggests the possibility of applying chain growth analysis methods similar to those developed by Herrington [42] to examine chain growth kinetics for the Fischer–Tropsch synthesis. The analysis becomes more complex for higher alcohol synthesis because chain growth occurs via several parallel pathways.

In order to apply these methods, chain termination probabilities for each chain size, (n) are obtained using the expression:

$$\beta_n \equiv r_{t,n}/r_{p,n} = \phi_n \Big/ \sum_{n=n+1}^{\infty} \phi_i, \qquad (7)$$

where ϕ_n is the mole fraction of chains of with n carbon atoms in the reactor effluent and $r_{t,n}$ and $r_{p,n}$ are the termination and propagation rates, respectively, for such chains with n-carbon atoms. The total termination probability ($\beta_{T,n}$) then becomes a linear combination of the values for the individual termination steps for all pathways leading to gas phase species with n carbon atoms:

$$\beta_{T,n} = \beta_{x,n} + \beta_{y,n} + \beta_{z,n}\ , \qquad (8)$$

where $\beta_{x,n}$ is the probability of termination via each distinct termination step, which can from the mole fraction of each species among reaction products using Eq. (7).

Both linear and aldol condensation chain growth by C_1 can occur during higher alcohol synthesis. These pathways lead to different products, except for the growth step from C_2 to C_3, in which both carbonylation and aldol-type C_1 addition lead to the same product (1-propanol). Self-condensation reactions of C_{2+} oxygenates, however, can also occur and they complicate the analysis.

As discussed above, linear chain growth is a minority pathway at the conditions of our study and it will be neglected in our chain growth analysis. Self-condensation of either ethanol or propanol, or ethanol with propanol, however, cannot be neglected. In our treatment, we will examine only the condensation steps described in Fig. 6. This analysis leads to the chain termination probabilities listed in Table 7 for Cs–Cu/ZnO/Al_2O_3, when 1-butanol and 2-methyl-1-pentanol are assumed to form only by self-condensation (of ethanol and propanol, respectively). 2-Methyl-1-butanol and 1-pentanol are assumed to form by condensation of ethanol with propanol. The formation of non-primary alcohols (except for 2-propanol) is negligible and it was not included in this analysis.

All chain growth probabilities on 2.9 wt% Cs–Cu/ZnO/Al_2O_3 increase with decreasing space velocity because longer bed-residence times and higher concentrations of intermediate products increases the probability for further chain growth reactions via readsorption and further chain growth of a C_n alcohol. Higher Cs concentrations lead to higher alcohol chain growth probabilities.

Table 8 shows chain growth probabilities for several $Cu_yMg_5CeO_x$ catalysts modified by K and Pd

Table 7
Chain growth probabilities for Cs–Cu/ZnO/Al_2O_3 (583 K, 4.5 MPa, H_2/CO=1)

Total chain growth probability	1.2 wt% Cs–Cu/ZnO/Al_2O_3	2.9 wt% Cs–Cu/ZnO/Al_2O_3	
Gas hourly space velocity (cm^3/g cat./h]	6000	6000	1500
CO conversion (%)	15.0	15.4	23.6
C_1 (to C_2)	0.05	0.10	0.17
C_2 (to C_3)	0.25	0.55	0.66
C_3 (to i-C_4)	0.23	0.38	0.56
i-C_4 (to neo-C_5)[a]	0	0	0

[a] Neo-pentanol (2,2-dimethyl-1-propanol) not detected.

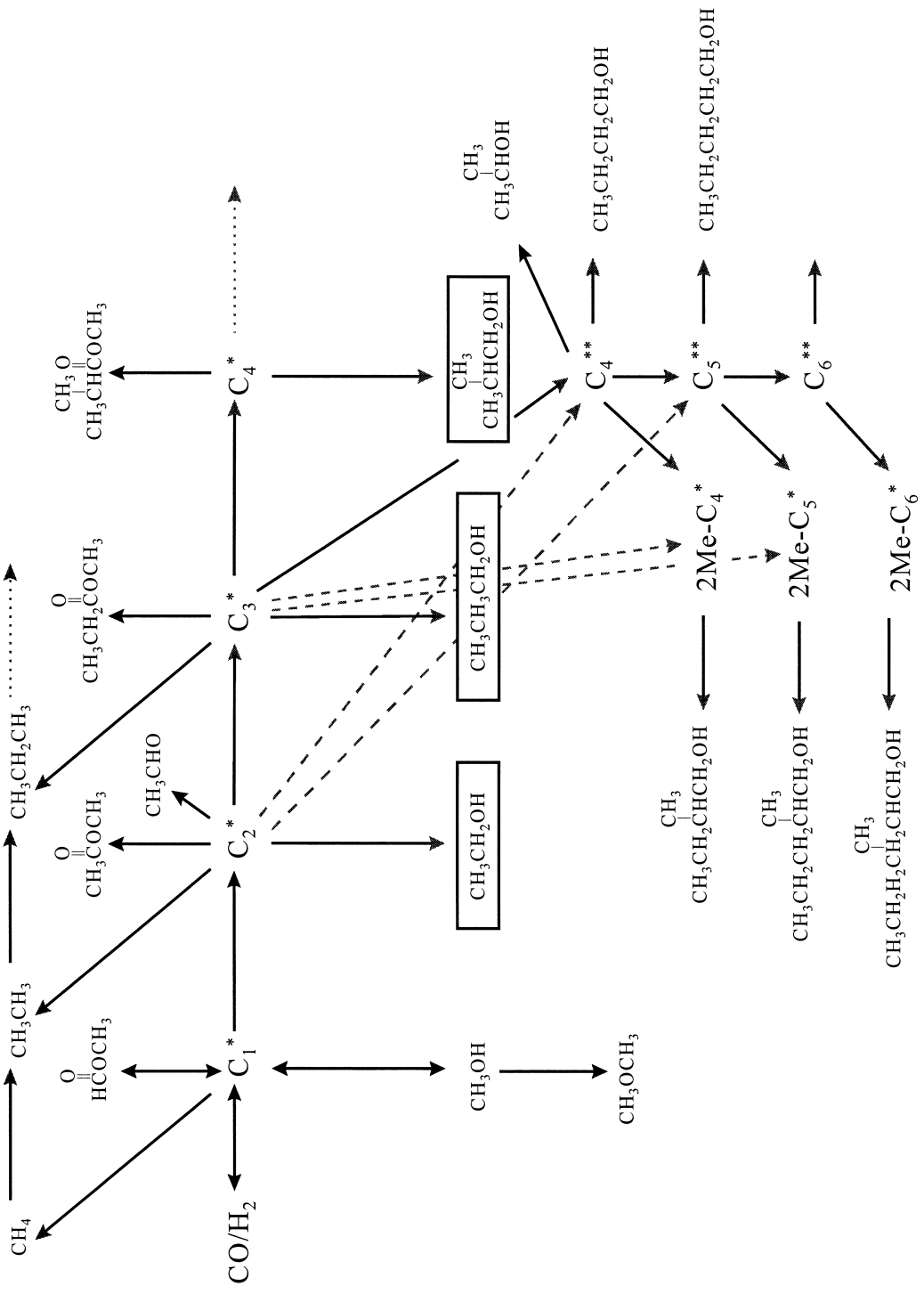

Fig. 5. Reaction network for methanol and higher alcohol synthesis with simultaneous formation of hydrocarbons.

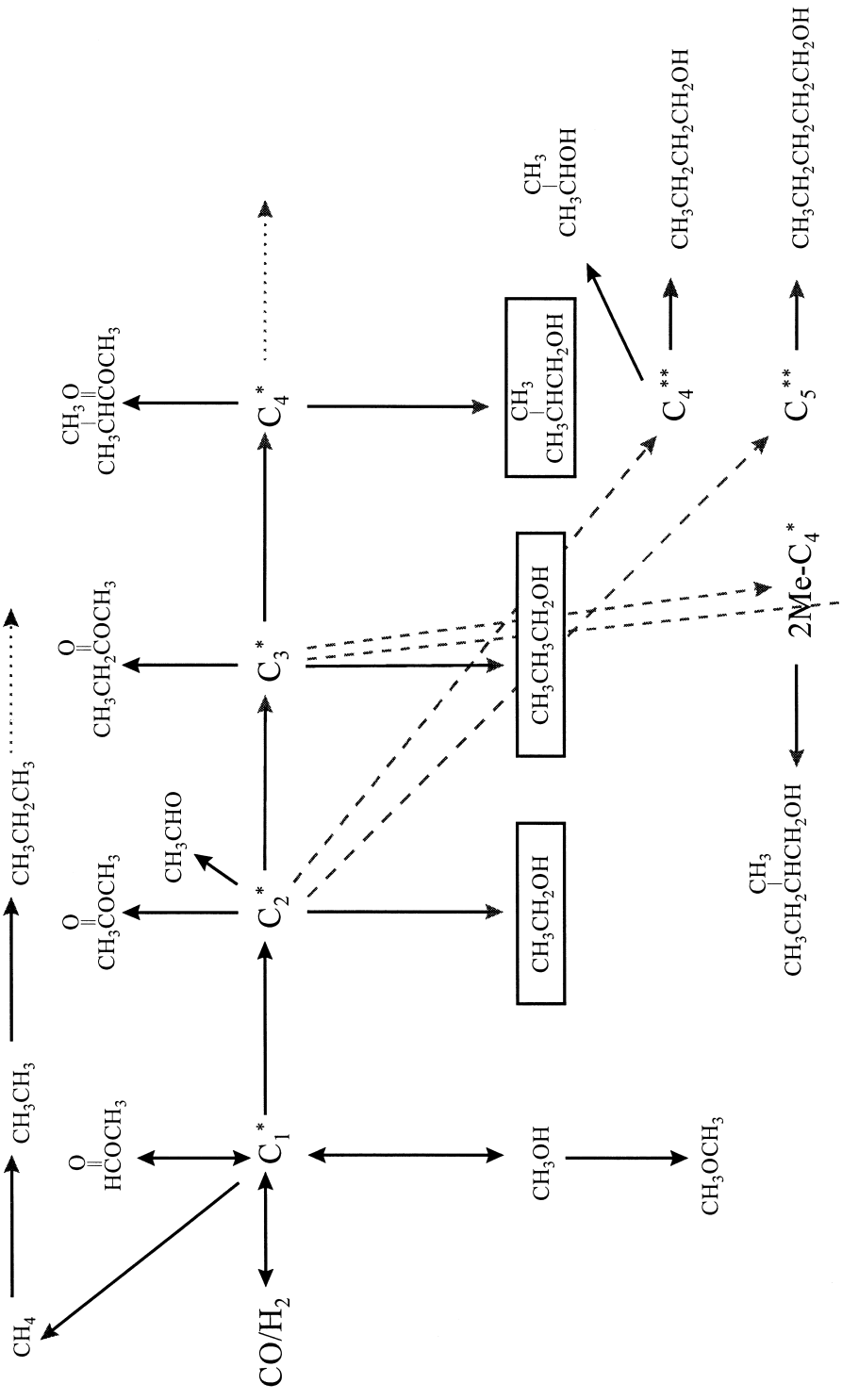

Fig. 6. Reaction network for methanol and higher alcohol synthesis without including linear chain growth pathways.

Table 8
Chain growth probabilities for K–$Cu_{0.5}Mg_5CeO_x$ and Cs–Cu/ZnO/Al_2O_3 (583 K, 4.5 MPa, H_2/CO=1)

Total chain growth probability	1 wt% K–$Cu_{0.5}Mg_5CeO_x$	0.25 wt% Pd 1 wt% K–$Cu_{0.5}Mg_5CeO_x$	1 wt% K–$Cu_{7.5}Mg_5CeO_x$	2.9 wt% Cs–Cu/ZnO/Al_2O_3
Gas hourly space velocity (cm^3/g cat/h)	1500	1500	6000	6000
CO conversion (%)	14.7	15.8	17.6	15.4
C_1 (to C_2)	0.07	0.09	0.08	0.10
C_2 (to C_3)	0.47	0.53	0.35	0.55
C_3 (to i-C_4)	0.54	0.50	0.27	0.38
i-C_4 (to neo-C_5)[a]	0	0	0	0

[a] Neo-pentanol (2,2-dimethyl-1-propanol) not detected.

Table 9
Chain growth probabilities before, and during alcohol addition on 2.9 wt% Cs–Cu/ZnO/Al_2O_3. (583 K, 4.5 MPa, 6000 cm^3/g cat/h, H_2/CO/Ar/C_2H_5OH =44.5/44.5/0.1/0.02, and H_2/CO/Ar/C_3H7OH =44.5/44.5/0.1/0.01)

Total chain growth probability	Molecule added to H_2/CO		
	none	ethanol	propanol
C_1 (to C_2)	0.10	—	—
C_2 (to C_3)	0.55	0.55	—
C_3 (to i-C_4)	0.38	0.32	0.45

compared at similar CO conversions. These catalysts show higher (C_3 to iC_4) chain growth values than Cs–Cu/ZnO/Al_2O_3 catalysts, but chain growth values are otherwise very similar to those on 2.9 wt% Cs–Cu/ZnO/Al_2O_3 for C_1 and C_2 species. K–$Cu_{7.5}Mg_5CeO_x$ shows lower chain growth values than similar catalysts containing lower Cu concentrations. This reflects a higher ratio of Cu to basic sites on these catalysts.

Table 9 shows chain growth probabilities when ethanol or propanol are added to the H_2/CO feed. No significant changes in chain growth probabilities were detected when alcohols were added, as expected from their participation only in chain initiation steps.

3.9. Comparison of K–$Cu_yMg_5CeO_x$ and Cu/ZnO/Al_2O_3 catalysts

Table 10 shows selectivities and isobutanol synthesis rates for 1 wt% K–$Cu_{0.5}Mg_5CeO_x$, 0.9 wt% K–

Table 10
Comparison of K–$Cu_yMg_5CeO_x$ and Cs–Cu/ZnO/Al_2O_3 catalysts (583 K, 4.5. MPa, H_2/CO=1)

Catalyst	1.0 wt% K–$Cu_{0.5}Mg_5CeO_x$	0.9 wt% K–$Cu_{7.5}Mg_5CeO_x$	1.2 wt% Cs–Cu/ZnO/Al_2O_3	2.9 wt% Cs–Cu/ZnO/Al_2O_3
Gas hourly space velocity (cm^3/g cat. h)	1500	6000	6000	6000
CO conversion (%)	14.7	17.6	15.0	15.4
Isobutanol rate (g/kg/h)	3.7	9.5	8.1	20.3
CO_2 selectivity (% C)	23.4	27.5	26.0	22.6
Carbon selectivities (%C; CO_2 free)				
Methanol	63.1	57.4	63.5	67.6
Ethanol	1.8	2.0	3.9	4.4
1-Propanol	3.0	3.1	2.3	6.9
2-Methyl-1-propanol	6.2	3.3	3.3	6.9
Methyl acetate	1.2	4.7	2.8	1.1
Dimethylether	6.8	0.7	7.0	0.8
Hydrocarbons	4.7	19.9	5.5	2.5
Isobutanol/methanol molar ratio	0.026	0.014	0.013	0.026
Surface Cu (mmol/g)	0.2175	0.5696	n.d.	0.3603
Turnover rates (mmol/mol Cu_s/s)				
Ethanol	0.03	0.08	—	0.27
1-Propanol	0.04	0.08	—	0.28
Isobutanol	0.06	0.06	—	0.21

$Cu_{7.5}Mg_5CeO_x$, 1.2 wt% Cs–Cu/ZnO/Al_2O_3, and 2.9 wt% Cs–Cu/ZnO/Al_2O_3 catalysts at similar conversions. The 2.9 wt% Cs–Cu/ZnO/Al_2O_3 catalyst showed the highest isobutanol synthesis rates at CO conversions of ca. 15%. Even on this catalyst, the molar ratio of isobutanol to methanol is only 0.03. Decreasing the space velocity increased this ratio to 0.1 (at 1500 cm^3/g/h) because methanol synthesis rates decrease with increasing bed-residence time due to thermodynamic constraints. K–$Cu_yMg_5CeO_x$ catalysts produce less isobutanol than Cs–Cu/ZnO/Al_2O_3 as a result of strong CO_2 inhibition on these catalysts at higher CO conversion, but isobutanol synthesis rates are similar to those on 2.9 wt% Cs–Cu/ZnO/Al_2O_3 at the low CO_2 concentrations characteristic of low CO conversions.

Turnover rates for ethanol, 1-propanol and isobutanol are also shown in Table 10. There appears to be no direct correlation between Cu surface area and alcohol synthesis rates. This is not surprising, because alcohol synthesis rates depend not only on Cu site density, but also on the density and strength of basic sites and on their interaction with CO_2 during alcohol synthesis reactions.

4. Conclusions

K–$Cu_yMg_5CeO_x$ and Cs–Cu/ZnO/Al_2O_3 were used for CO hydrogenation reactions to form higher alcohols. K-promoted $Cu_{0.5}Mg_5CeO_x$ catalysts are active catalysts for isobutanol synthesis from CO/H_2 mixtures and give products with high alcohol-to-hydrocarbon ratios at relatively low temperatures (583 K) and pressures (4.5 MPa). Cs-promoted Cu/ZnO/Al_2O_3 catalysts show higher isobutanol synthesis rates than K–$Cu_yCeMg_5O_x$ catalysts at high conversion conditions, but synthesis rates become similar at low CO conversions. CO_2 strongly inhibits methanol and isobutanol synthesis rates on catalysts with low Cu concentration (K–$Cu_{0.5}Mg_5CeO_x$). Methanol synthesis rates were not affected by CO_2 on catalysts with high Cu content (K–$Cu_{7.5}Mg_5CeO_x$ and Cs–Cu/ZnO/Al_2O_3), because they typically operate at methanol synthesis equilibrium. Isobutanol synthesis was more severely inhibited by CO_2 on K–$Cu_{7.5}Mg_5CeO_x$ than on Cs–Cu/ZnO/Al_2O_3, apparently as a result of the presence of stronger basic sites on the former. The addition of small amounts of Pd to K–$Cu_{0.5}Mg_5CeO_x$ weakens the adverse effects of CO_2, probably because Pd resists oxidation and retains its hydrogenation activity at high CO_2 partial pressures. The addition of K (or Cs) to $Cu_yMg_5CeO_x$ (or Cu/ZnO/Al_2O_3) samples titrates residual acid sites, which lead to dimethylether and hydrocarbons. Ethanol and 1-propanol addition data show that predominant chain growth pathways are aldol-type C_1 addition to C_{2+} alcohols on both K–$Cu_yMg_5CeO_x$ and Cs–Cu/ZnO/Al_2O_3. A chain growth analysis showed only minor differences in chain growth probabilities between the two types of catalysts examined in this study. This analysis also confirmed the role of alcohols as chain initiators during higher alcohol synthesis.

Acknowledgements

This work was supported by the Division of Fossil Energy of the United States Department of Energy under Contract Number DE-AC22-94PC94066. A.-M. Hilmen acknowledges the Norwegian Research Council for a post-doctoral fellowship. M.J.L. Gines acknowledges the Universidad Nacional del Litoral, Santa Fe, Argentina for a post-doctoral fellowship. The authors also express their thanks to Drs. Bernard Toseland and Richard Underwood of Air Products and Chemicals, Inc. for helpful suggestions and technical discussions.

References

[1] P. Forzatti, E. Tronconi, I. Pasquon, Cat. Rev. Sci. Eng. 33(1)&2 (1991) 109.
[2] G. Natta, U. Colombo, I. Pasquon, in P.H. Emmet (Ed.), Catalysis, vol. V, Chap. 3, Reinhold, New York, 1957, p. 131.
[3] K.J. Smith, R.B. Anderson, Can. J. Chem. Eng. 61 (1983) 40.
[4] G.A. Vedage, P.B. Himelfarb, G.W. Simmons, K. Klier, ACS Symp. Ser. 279 (1985) 295.
[5] J.G. Nunan, C.E. Bogdan, K. Klier, K.J. Smith, C.-W. Young, R.G. Herman, J. Catal. 116 (1989) 195.
[6] B.B. Breman, A.C.C.M. Beenackers, E. Oesterholt, Chem. Eng. Sci. 49 (1994) 4409.
[7] B.B. Breman, A.C.C.M. Beenackers, E. Oesterholt, Catal. Today 24 (1995) 5.
[8] E.M. Calverley, R.B. Anderson, J. Catal. 104 (1987) 434.
[9] E.M. Calverley, K.J. Smith, J. Catal. 130 (1991) 616.

[10] E.M. Calverley, K.J. Smith, Ind. Eng. Chem. Res. 31 (1992) 792.
[11] D.J. Elliott, F. Pennella, J. Catal. 114 (1988) 90.
[12] D.J. Elliott, F. Pennella, J. Catal. 119 (1989) 359.
[13] D.J. Elliott, J. Catal. 111 (1988) 445.
[14] A. Kiennemann, H. Idriss, R. Keiffer, P. Chaumette, D. Durand, Ind. Eng. Chem. Res. 30 (1991) 1130.
[15] J.C. Slaa, J.G. van Ommen, J.R.H. Ross, Catal. Today 15 (1992) 129.
[16] K.J. Smith, R.B. Anderson, J. Catal. 85 (1984) 428.
[17] K. Klier, V. Chatikavanij, R.G. Herman, G.W. Simmons, J. Catal. 74 (1982) 343.
[18] J.G. Nunan, K. Klier, C.-W. Young, P.B. Himelfarb, R.G. Herman, J. Chem. Soc. Chem. Commun. 193 (1986).
[19] K. Klier, R.G. Herman, J.G. Nunan, K.J. Smith, C.E. Bogdan, C.-W. Young, J.G. Santiesteban, in D.M. Bibby, C.D. Chang, R.F. Howe, S. Yurchak (Eds.), Methane Conversion, Elsevier, Amsterdam, vil. 188, 1988, p. 109.
[20] J.G. Nunan, C.E. Bogdan, K. Klier, K.J. Smith, C.-W. Young, R.G. Herman, J. Catal. 113 (1988) 410.
[21] J.G. Nunan, C.E. Bogdan, R.G. Herman, K. Klier, Catal. Lett. 2 (1989) 49.
[22] J.G. Nunan, R.G. Herman, K. Klier, J. Catal. 116 (1989) 222.
[23] K.J. Smith, C.-W. Young, R.G. Herman, K. Klier, Ind. Eng. Chem. Res. 30 (1991) 61.
[24] J.M. Campos-Martín, J.L.G. Fierro, A. Guerrero-Ruiz, R.G. Herman, K. Klier, J. Catal. 163 (1996) 418.
[25] A. Beretta, Q. Sun, R.G. Herman, K. Klier, Ind. Eng. Chem. Res. 35 (1996) 1534.
[26] C.R. Apesteguia, S. Soled, S. Miseo, US Patent 5,387, 570 (1993), assigned to Exxon Research and Engineering Co.
[27] C.R. Apesteguia, B. De Rites, S. Miseo, S. Soled, Catal. Lett. 44 (1997) 1.
[28] W. Keim, W. Falter, Catal. Lett. 3 (1989) 59.
[29] E. Tronconi, P. Forzatti, I. Pasquon, J. Catal. 124 (1990) 376.
[30] J.L. Robbins, E. Iglesia, C.P. Kelkar, B. De Rites, Catal. Lett. 10 (1991) 1.
[31] G.C. Chinchen, K.C. Waugh, D.A. Whan, Appl. Catal. 25 (1986) 101.
[32] M. Xu, E. Iglesia, Catal. Lett., in press.
[33] M.J.L Gines, E. Iglesia, J. Catal., in press.
[34] M. Xu, M.J.L. Gines, A.M. Hilmen, B.L. Stephens, E. Iglesia, J. Catal. 171 (1997) 130.
[35] G.C. Chinchen, P.J. Denny, J.R. Jennings, M.S. Spencer, K.C. Waugh, Appl. Catal. 36 (1988) 1.
[36] J.-L. Li, T. Inui, Appl. Catal. 137 (1996) 105.
[37] E. Iglesia, M. Boudart, J. Catal. 81 (1983) 204.
[38] K. Narita, N. Takezawa, I. Toyoshima, React. Kinet. Catal. Lett. 19 (1982) 91.
[39] M. Xu, E. Iglesia, J. Phys. Chem. 102 (1998) 961.
[40] E. Tronconi, N. Ferlazzo, P. Forzatti, I. Pasquon, Ind. Eng. Chem. Res. 26 (1987) 2122.
[41] N.W. Hurst, S.J. Gentry, A. Jones, B. McNicol, Catal. Rev.-Sci. Eng. 24(2) (1982) 233.
[42] E.F.G. Herrington, Chem. Ind. 102 (1946) 346.